Distinct In Vitro Properties of Embryonic and Extraembryonic Fibroblast-Like Cells Are Reflected in Their In Vivo Behavior Following Grafting in the Adult Mouse Brain

Peer-reviewed author version

Costa, Roberta; Bergwerf, Irene; SANTERMANS, Eva; De Vocht, Nathalie; Praet, Jelle; Daans, Jasmijn; Le Blon, Debbie; Hoomaert, Chloe; Reekmans, Kristien; HENS, Niel; Goossens, Herman; Berneman, Zwi; Parolini, Ornella; Alviano, Francesco & Ponsaerts, Peter (2015) Distinct In Vitro Properties of Embryonic and Extraembryonic Fibroblast-Like Cells Are Reflected in Their In Vivo Behavior Following Grafting in the Adult Mouse Brain. In: CELL TRANSPLANTATION, 24 (2), p. 223-233.

DOI: 10.3727/096368913X676196
Handle: http://hdl.handle.net/1942/18719

CELL TRANSPLANTATION
The Regenerative Medicine Journal

Distinct in vitro properties of embryonic and extra-embryonic fibroblast-like cells are reflected in their in vivo behaviour following grafting in the adult mouse brain.

Journal:	*Cell Transplantation*
Manuscript ID:	CT-1128.R1
Manuscript Type:	Original Article
Date Submitted by the Author:	n/a
Complete List of Authors:	Costa, Roberta Bergwerf, Irene Santermans, Eva De Vocht, Nathalie Praet, Jelle Daans, Jasmijn Le Blon, Debbie Hoornaert, Chloé Reekmans, Kristien Hens, Niel Goossens, Herman Berneman, Zwi; University of Antwerp, Experimental Hematology Parolini, Ornella Alviano, Francesco Ponsaerts, Peter; University of Antwerp, Experimental Hematology
Keywords:	Foetal membrane-derived stromal cells, embryonic fibroblasts, immunomodulation, transplantation, angiogenesis
Abstract:	Although intracerebral transplantation of various fibroblast(-like) cell populations has been shown feasible, little is known about the actual in vivo remodelling of these cellular grafts and their environment. In this study, we aimed to compare the in vitro and in vivo behaviour of two phenotypically similar - but developmentally distinct - fibroblast-like cell populations, namely mouse embryonic fibroblasts (mEF) and mouse foetal membrane-derived stromal cells (mFMSC). While both mEF and mFMSC are readily able to reduce TNFα secretion by LPS/IFNγ-activated BV2 microglia, mFMSC and mEF display a strikingly opposite behaviour with regard to VEGF production under normal and inflammatory conditions. Whereas mFMSC downregulate VEGF production upon co-culture with LPS/IFNγ-activated BV2 microglia, mEF upregulate VEGF production in the presence of LPS/IFNγ-activated BV2 microglia. Subsequently, in vivo grafting of mFMSC and mEF revealed no difference in microglial and astroglial responses towards the cellular grafts. However, mFMSC grafts displayed a lower degree of neo-angiogenesis as compared to mEF grafts, thereby potentially explaining the lower cell number able to survive in mFMSC grafts. In summary, our results suggest that physiological

	differences between fibroblast-like cell populations might lie at the basis of variations in histopathological and/or clinical outcome following cell grafting in mouse brain.

Distinct in vitro properties of embryonic and extra-embryonic fibroblast-like cells are reflected in their in vivo behaviour following grafting in the adult mouse brain.

Roberta Costa[1], Irene Bergwerf[2,3], Eva Santermans[4], Nathalie De Vocht[2,3], Jelle Praet[2,3], Jasmijn Daans[2,3], Debbie Le Blon[2,3], Chloé Hoornaert[2,3], Kristien Reekmans[2,3], Niel Hens[4,5], Herman Goossens[3], Zwi Berneman[2,3], Ornella Parolini[6], Francesco Alviano[1] and Peter Ponsaerts[2,3]

[1] Department of Experimental, Diagnostic and Specialty Medicine, University of Bologna, Bologna, Italy.

[2] Experimental Cell Transplantation Group, Laboratory of Experimental Hematology, University of Antwerp, Antwerp, Belgium.

[3] Vaccine and Infectious Disease Institute (Vaxinfectio), University of Antwerp, Antwerp, Belgium.

[4]Center for Statistics, I-Biostat, Hasselt University, Hasselt, Belgium.

[5]Centre for Health Economic Research and Modeling Infectious Diseases (Chermid), University of Antwerp, Antwerp, Belgium.

[6] Centro di Ricerca E. Menni, Fondazione Poliambulanza – Istituto Ospedaliero, Brescia, Italy.

Running head: differential in vivo behaviour of cellular grafts

Corresponding author:

prof. dr. Peter Ponsaerts, Experimental Cell Transplantation Group, Laboratory of Experimental Hematology, Vaccine and Infectious Disease Institute (Vaxinfectio), University of Antwerp, Campus Drie Eiken (CDE-S6.51), Universiteitsplein 1, 2610 Antwerp (Wilrijk), Belgium. Tel.: 0032-3-2652428 - E-mail: peter.ponsaerts@uantwerpen.be

Abstract:

Although intracerebral transplantation of various fibroblast(-like) cell populations has been shown feasible, little is known about the actual *in vivo* remodelling of these cellular grafts and their environment. In this study, we aimed to compare the *in vitro* and *in vivo* behaviour of two phenotypically similar - but developmentally distinct - fibroblast-like cell populations, namely mouse embryonic fibroblasts (mEF) and mouse foetal membrane-derived stromal cells (mFMSC). While both mEF and mFMSC are readily able to reduce TNFα secretion by LPS/IFNγ-activated BV2 microglia, mFMSC and mEF display a strikingly opposite behaviour with regard to VEGF production under normal and inflammatory conditions. Whereas mFMSC downregulate VEGF production upon co-culture with LPS/IFNγ-activated BV2 microglia, mEF upregulate VEGF production in the presence of LPS/IFNγ-activated BV2 microglia. Subsequently, *in vivo* grafting of mFMSC and mEF revealed no difference in microglial and astroglial responses towards the cellular grafts. However, mFMSC grafts displayed a lower degree of neo-angiogenesis as compared to mEF grafts, thereby potentially explaining the lower cell number able to survive in mFMSC grafts. In summary, our results suggest that physiological differences between fibroblast-like cell populations might lie at the basis of variations in histopathological and/or clinical outcome following cell grafting in mouse brain.

Key words:

Foetal membrane-derived stromal cells, embryonic fibroblasts, immunomodulation, transplantation, brain, angiogenesis

INTRODUCTION

Transplantation of fibroblastic cells, including adult/embryonic fibroblasts and mesenchymal stromal cells, is widely being applied in various preclinical animal models of human disease. Major interest into these cell populations can be explained by the relatively easy *in vitro* isolation (and/or expansion) protocols and the exceptional immune-modulating and regeneration-inducing properties of these cells (2). However, while extensive *in vitro* experiments have shed light on potential working mechanisms for the improved clinical outcome following fibroblastic cell grafting in several disease models, including those of the central nervous system (CNS), currently little is known about the actual *in vivo* behaviour of these cellular grafts (1,7). In our preceding studies, we contributed to a better understanding of the cellular events following syngeneic reporter gene-modified murine bone marrow-derived mesenchymal stromal cell (mMSC) and murine embryonic fibroblast (mEF) grafting in the healthy and injured CNS of immune-competent mice (4,5,10,21). In course of these studies, it was noted that both mMSC and mEF grafting in the CNS, independent of a preceding injury, results in the activation of strong microglial and astroglial cell responses. Without manifest differences, both mMSC and mEF grafts become highly surrounded and infiltrated with Iba1+ microglia(/macrophages). In addition, both mMSC and mEF grafts become surrounded, but not infiltrated, by highly activated GFAP+ astrocytes. Given the *in vivo* occurrence of cellular immune responses against grafted fibroblastic cells, although we do not yet know the exact mechanism behind, further research towards identifying a cell population that triggers no or minimal CNS immune responses upon transplantation is highly desirable. The latter will not only lead to the application of safer therapeutic cell-based therapies, but more importantly, might lead to the establishment of therapeutic interventions in which functional cell integration might occur in the adult immune competent CNS (5).

Recently, the placenta, foetal membranes and amniotic fluid have been put forward as alternative

sources for cells of mesenchymal origin in cell transplantation experiments (16,29). Based on the observation that during pregnancy the competent immune system of the mother is rendered tolerant to the immunologically distinct foetus, the placenta and foetal membranes, which are the interface between mother and foetus, may harbour these immune regulating properties. The hypothesis that foetal membranes are a non immunogenic tissue has been confirmed by several clinical studies that used amniotic membranes for treatment of skin wounds, dermal burns, non-healing ulcers, ocular surface reconstruction, or to prevent tissue adhesion in surgical procedures (12,16). In these clinical studies, no immune-mediated rejection was observed in the absence of immune suppressive treatment. Moreover, fibroblast-like cells isolated from foetal membranes, generally termed foetal membrane-derived stromal cells (FMSC), can present the same immunological behaviour. In this context, several preclinical studies in animal models of disease demonstrated that transplantation of human (h)FMSC significantly contributes to anti-inflammatory and anti-scarring processes rather than actual cell replacement. For example, hFMSC transplantation for the treatment of liver and lung fibrosis in rodents showed a reduction in neutrophil infiltration and in the dimension of the fibrotic lesion (8,17). This immunological behaviour of hFMSC has also been observed following neural injury. Transplantation of hFMSC after stroke in rodents has shown to reduce injury progression by modulating the inflammatory response and facilitating functional recovery (16,19). Furthermore, other *in vivo* experiments have demonstrated long-term survival of hFMSC after xenogeneic transplantation into immune competent animals (12,14).

However, despite demonstrating significant immune modulating effects, the xenogeneic transplantation of human cells into rodents has significant limitations when aiming to translate the observed clinical benefits to human clinical applications that will be performed with autologous or allogeneic cell grafts. Therefore, in this novel study we first optimised an isolation procedure for murine (m)FMSC and characterised the resulting mFMSC population *in vitro* and *in vivo* following

syngeneic grafting in the CNS. Comparing the obtained data with a mEF control cell population, this study describes functional differences between fibroblast-like cell populations isolated from different tissues, both *in vitro* and *in vivo* upon grafting in the CNS.

MATERIALS AND METHODS

Animals

Female wild type C57BL/6 mice (Charles River Laboratories, strain code 027) were crossed with male transgenic C57BL/6-eGFP mice (Jackson Laboratories, strain code 003291) and both eGFP+ and eGFP- embryos/foetal membranes were used for cell isolation experiments. Male wild type C57BL/6 mice (Charles River Laboratories, strain code 027), 8-9 weeks of age, were used for cell implantation experiments (n=10). For all experiments, mice were kept under normal day-night cycle (12-12) with free access to water and food. All experimental procedures were approved by the ethical committee for animal experiments of the University of Antwerp (approval n. 2011-13).

Cell culture

mFMSC were isolated from eGFP+ and eGFP- foetal membranes surrounding respectively eGFP+ and eGFP- embryos following crossing of female wild type C57BL/6 mice with male transgenic C57BL/6-eGFP mice. For this, embryos (E17-18) were removed from the uterus and each foetal membrane was separated manually from the placenta and the embryo. Foetal membranes were recovered, washed with PBS (Gibco) and enzymatically digested by the following consecutive dissociation steps: 3 minutes in PBS supplemented with Dispase (2.5 U/ml, Gibco), 3 hours in RPMI medium (Gibco) supplemented with Collagenase A (1.5 mg/ml, Roche) and DNAse I (0.002 mg/ml, Sigma), and 3 minutes in 0.05% Trypsin-EDTA (Invitrogen). The cell suspension obtained was then plated in 6 well plates (Corning) at a cell density of 7-9x10^4 cells/cm^2 (one well for each foetal membrane) in RPMI medium supplemented with 10% foetal calf serum (FCS, Hyclone), 100 U/ml Penicillin (Invitrogen) and 100 mg/ml Streptomycin (Invitrogen). For cell expansion and to establish a growth curve, cell culture medium was replaced every 3 days and cells were split 1:2 and counted every 4 days. mEF were cultured from eGFP+ and eGFP- embryos following crossing of female wild

type C57BL/6 mice with male transgenic C57BL/6-eGFP mice, according to previously described procedures (21). For cell expansion, mEF medium (DMEM (with 4.5 g/L glucose and L-glutamine, Gibco) supplemented with 10% FCS, 100 U/ml Penicillin and 100mg/ml Streptomycin) was replaced every 2-3 days and cells were split 1:3 every 4-5 days. In order to establish a growth curve, mEF cultures were plated at $9x10^4$ cells/cm^2, split 1:2 and counted every 4 days. BV2 microglial cells (kindly provided by prof. R. Donato, University of Perugia, Italy) were cultured in DMEM supplemented with 10% FCS, 100 U/ml Penicillin and 100mg/ml Streptomycin. For cell culture, BV2 medium was replaced every 2 days and cells were split 1:5 every 3 days. All cell cultures were incubated in a humidified incubator at 37°C with 5% CO_2.

Flow cytometric analysis

Immunophenotyping of eGFP- mFMSC and eGFP- mEF cell populations was performed using the following directly labelled antibodies: phycoerythrin (PE)-labelled rat anti mouse Sca1 (R&D, FAB1226P), PE-labelled mouse anti mouse CD90 (eBioscience, 12-0900-81), PE-labelled rat anti mouse CD44 (eBioscience, 12-0441-81), PE-labelled rat anti mouse MHC class II (eBioscience, 12-5321-82), PE-labelled rat anti mouse CD184 (BD, 551966), PE-labelled mouse anti mouse H2Kb (BD 553570), fluorescein (FITC)-labelled rat anti mouse CD45 (eBioscience 11-0451-82), FITC-labelled rat anti mouse CD106 (eBioscience, 11-1061-82), FITC-labelled rat anti mouse CD31 (eBioscience, 11-0311-82), FITC-labelled rat anti mouse CD4 (eBioscience, 11-0041-82), FITC-labelled rat anti mouse CD8a (eBioscience, 11-0081-82), FITC-labelled rabbit anti mouse TGFβ RII (Santa Cruz, sc-1700). Before staining, harvested cells were washed twice with PBS and suspended in PBS at a concentration of 2×10^6 cells/ml. For antibody staining, 1 µg of antibody was added to 100 µl of cell suspension for 30 min at 4°C. Following incubation, cells were washed once with PBS, suspended in 1 mL PBS, and analysed by flow cytometry. For detection of eGFP transgene expression, harvested eGFP+ mFMSC and eGFP+ mEF were washed once with PBS, suspended in PBS and directly

analysed by flow cytometry. For all analyses, cell viability was assessed by adding GelRed (1× final concentration, Biotum) to the cell suspension immediately before flow cytometric analyis. All flow cytometric analyses were performed using an Epics XL-MCL analytical flow cytometer (Beckman Coulter) and all data were analysed using FlowJo flow cytometry data analysis software (FlowJo).

Cell differentiation assays

For adipogenic differentiation, mFMSC and mEF were plated at $2x10^4$ cells/cm^2 in 24 well plates (Corning) followed by culture in Mesenchymal Stem Cell Adipogenic Differentiation Medium (PT 3004, Lonza), according to the manufacturer's instructions. Control non-induced cells were kept in basal medium (RPMI 10% FCS for mFMSC and DMEM 10% FCS for mEF). After 3 weeks of culture, cells were fixed with 4% paraformaldehyde and stained with fresh Oil Red O solution (Sigma). For osteogenic differentiation, mFMSC and mEF were plated at $1x10^4$ cells/cm^2 in 24 well plates followed by culture in Mesenchymal Stem Cell Osteogenic Differentiation Medium (PT 3002, Lonza), according to the manufacturer's instructions. Control non-induced cells were kept in basal medium. After 3 weeks of culture, cells were fixed with 4% paraformaldehyde (Sigma) and stained with Alizarin Red S (Sigma). For chondrogenic differentiation, $2.5x10^5$ mFMSC or mEF were pelleted in 15 ml conical tubes (Greiner) followed by culture in Mesenchymal Stem Cell Chondrocyte Differentiation Medium (PT 3003, Lonza) supplemented with TGFβ 3 (Sigma), according to the manufacturer's instructions. Control non-induced cells were kept in basal medium after pelleting. After 3 weeks of induction, cells were fixed with 4% paraformaldehyde and stained with Alcian Blue (Sigma).

mFMSC and mEF co-culture experiments with BV2 cells

mFMSC and mEF were plated at a concentration of $5x10^4$ cells/well in a 24 well plate and allowed to adhere during overnight incubation. Next, in order to assess the effect of mFMSC and mEF on BV2

microglial cells, $1x10^5$ BV2 cells were plated onto the confluent layer of mFMSC or mEF. Following 24 hours of co-culture, cultures were additionally stimulated with lipopolysaccharide (LPS, Invivogen, 1μg/ml) + interferon-γ (IFNγ) (R&D Systems, 500U/ml) to assess the effect of mFMSC and mEF on activated BV2 microglial cell (28). After an additional 24 hours of stimulation (or under control conditions) supernatants was harvested and analysed for the presence of TNFα and VEGF by means of ELISA, according to the manufacturer's instructions (murine TNFα ELISA from Biolegend, murine VEGF ELISA from Peprotech).

Cell implantation experiments

Cell implantation in the CNS of immune competent mice was performed under sterile conditions according to previously established procedures (10,21,24). Briefly, eGFP-expressing mFMSC and mEF were harvested, washed with PBS and resuspended at a concentration of approximately $41.6x10^6$ cells / ml in PBS. Directly prior to and post transplantation, the cell number was recounted in order to control for the actual number of injected cells ($5x10^4$ cells in 1.2 μl PBS). For cell implantation, mice were anesthetized by an intraperitoneal injection of a ketamin (80 mg/kg, Pfizer) + xylazin (16 mg/kg, Bayer Health care) mixture in PBS and placed in a stereotactic frame (Stoelting). Next, a midline scalp incision was made and a hole was drilled in the skull using a dental drill burr (Stoelting) at the following coordinates relative to bregma: 0.5 mm posterior and 2.2 mm lateral to the right side of the midline. Thereafter, an automatic microinjector pump (kdScientific) with a 10-μl Hamilton syringe was positioned above the exposed dura. A 30-gauge needle (Hamilton), attached to the syringe, was stereotactically placed through the intact dura to a depth of 3.3 mm. After 2 min of pressure equilibration, 5×10^4 cells of the respective populations were injected in a volume of 1.2 μl PBS at a speed of 0.7 μl/min. The needle was retracted after another 4 min to allow pressure equilibration and to prevent backflow of the injected cell suspension. Next, the skin was sutured (Vicryl, Ethicon) and a

0.9% NaCl solution (Baxter) was administered subcutaneously in order to prevent dehydration while mice were placed under a heating lamp to recover.

Histological analysis – immunofluorescence staining

Preparation of brain tissue for histological examination was performed according to previously optimised procedures (10,21,22). Serial 10-µm thick cryosections were obtained from the entire implant region using a Microm HM5000 cryostat (Prosan), consecutively marked and missing slides were noted. For further immunofluorescence analysis of tissue sections, antibody staining was performed as previously described (10,21,22) using the following antibodies: (i) a rabbit anti-mouse Iba1 antibody (Wako 019-19741, 1/400 dilution) in combination with an Alexa Fluor® 555-labelled donkey anti-rabbit secondary antibody (Invitrogen A31572, 1/1000 dilution), (ii) a mouse anti-mouse GFAP antibody (Millipore mab377, 1/400 dilution) in combination with an Alexa Fluor® 350-labelled goat anti-mouse secondary antibody (Invitrogen A11068, 1/200 dilution), (iii) a rabbit anti-mouse S100b antibody (Abcam ab52642, 1/400 dilution) in combination with an Alexa Fluor® 555-labelled donkey anti-rabbit secondary antibody (Invitrogen A-31572, 1/1000 dilution), (iv) a rabbi anti-mouse CD31 antibody (Abcam AB28364, 1/50 dilution) in combination with a Texas Red-labelled goat anti-rabbit secondary antibody (Abcam AB6719, 1/1000 dilution). Antibody stainings were performed using the following single or double staining combinations: (i) Iba1 (n = 2 per cell grafted mouse brain), (ii) S100b + GFAP (n = 2 per cell grafted mouse brain), (iii) CD31 (n = 1 per cell grafted mouse brain). In brief, slides were rinsed for 5 min in Tris-buffered saline (TBS) and subsequently incubated for 30 min in 0.1% Triton-X (Merck) in TBS. Next, slides were washed, followed by a 1 hour incubation at room temperature in TBS + blocking serum (for Iba-1 staining TBS + 20% donkey serum from Jackson ImmunoResearch (017-000-121); for S100b/GFAP staining TBS + 20% donkey serum, 20% goat serum from Jackson ImmunoResearch (005-000-121) and 1% unconjugated goat anti-mouse Ig from Jackson ImmunoResearch (115-007-003); for CD31 staining TBS + 20% goat

serum). Next, blocking solution was removed and slides were incubated overnight at 4°C with the primary antibodies diluted in TBS + 10% (w/v) milk powder. Next, slides were washed with TBS (4 x 3 min) and incubated for 1 h at room temperature on a horizontal shaker (at 60 rpm) with the secondary antibodies diluted in TBS + 10% (w/v) milk powder. Thereafter, slides were washed with TBS (4 x 3 min) and a 20 min nuclear staining was performed using Topro-3 (Invitrogen, T3605, 1/200 dilution). Following final washing with TBS (3 x 2 min), stained slides were mounted using Prolong Gold Antifade Reagent (Invitrogen, P36930) and images were acquired using an Olympus BX51 microscope equipped with an Olympus DP71 digital camera. Olympus CellSense software was used for image acquisition.

Histological analysis – quantitative analysis

Quantitative analysis of cell graft survival, glial cell responses and angiogenesis was performed using NIH ImageJ analysis software (ImageJ) and TissueQuest immunofluorescence analysis software (TissueGnostics GmbH) as previously described (10,22), allowing determination of the following parameters: (i) the mFMSC/mEF graft site volume in mm^3 (1 data count per cell graft analysed), (ii) the density (in cells/mm^3) and absolute number of eGFP+ mFMSC/mEF within the graft site (4 estimates per cell graft analysed), (iii) the mFMSC/mEF cell graft survival provided in absolute numbers and in % calculated to the initial number of grafted eGFP+ viable mFMSC/mEF (4 estimates per cell graft analysed), (iv) the density (in cells/mm^3) and absolute number of Iba1+ microglia within the mFMSC/mEF graft site (4 estimates per cell graft analysed), (v) the density (in cells/mm^3) of Iba1+ microglia within the mFMSC/mEF graft site border, as determined by a region extending 100 µm from the mFMSC/mEF graft site (2 estimates per cell graft analysed), (vi) the density (in cells/mm^3) of S100b+ astrocytes within the mFMSC/mEF graft site border (2 estimates per cell graft analysed), (vii) the degree of GFAP+ astrogliosis within the mFMSC/mEF graft site border provided as % astrogliosis (2 estimates per cell graft analysed), and (viii) the density (in cells/mm^2) of CD31+

blood vessels within the mFMSC/mEF graft (one data count per cell graft analysed).

Statistical analyses

All statistical analyses were performed using the IBM SPSS version 20 statistical package. To examine differences in *in vitro* cell growth (day 0, day 4 and day 8 post-plating) between mFMSC and mEF cultures, a mixed model with repeated measures and a first-order autoregressive covariance structure was fitted. To evaluate differences in *in vitro* TNF-α/VEGF secretion, both outcomes were first transformed using an inverse-logistic equation. A one-way ANOVA was then performed on these transformed variables and several post-hoc tests were used to assess statistically significant differences (highest p-value is reported). To evaluate differences in graft site volume, total cell number within the graft site, number of eGFP+ cells within the graft site, % cell graft survival, ratio microglia vs. eGFP+ cells within the graft site, density of microglia in the graft site surrounding, density of astrocytes in the graft site surrounding, % of astrogliosis and density of blood vessels within the graft site, Generalized Estimating Equations (30) taking into account repeated measures were used. This method does not require a priori specification of the association structure. The obtained p-values were corrected using the false-discovery rate control (3). For all comparisons, a p-value < 0.05 was considered to be statistically significant.

RESULTS

Phenotypical characterisation of mFMSC and mEF cultures

mFMSC and mEF were isolated from wild-type C57BL/6 mice or from transgenic C57BL/6-eGFP mice, as described in the materials and methods section. As shown in figure 1A (a+b, main images), both mFMSC and mEF are adherently cultured cell populations displaying a typical fibroblast-like morphology. When mFMSC-eGFP and mEF-eGFP were isolated from C57BL/6-eGFP transgenic mice, both cell populations uniformly displayed high eGFP expression as measured by flow cytometry (figure 1A, a+b, inset images). Further flow cytometric immunophenotyping of mFMSC and mEF characterised both cell populations as follows: Sca1+, CD44+, CD90+ (low), CD31-, CD106-, CD45-, CD184-, CD4-, CD8-, TGFβRII-, MHCI- and MHCII+ (low) (figure 1A, c+d). Of note, these embryonic stromal cell populations are phenotypically slightly different from adult C57BL/6 murine bone marrow-derived mesenchymal stromal cells (mBMMSC), as the latter were previously characterised as: Sca1+ (high), CD44+ (high), CD90-, CD31-, CD106-, CD45-, CD184-, CD4-, CD8-, TGFβRII-, MHCI+ (low) and MHCIl+ (low), implying small phenotypic variations between fibroblast-like cell types derived from adult or embryonic tissues (data not shown).

Functional characterisation of mFMSC and mEF

First, we evaluated the proliferative capacity of the isolated mFMSC and mEF cell populations (figure 1B). While mEF cultures can easily be expanded *in vitro* ($p<0.001$), mFMSC did not display any proliferation. Moreover, in the current setup, we were unable to maintain mFMSC in culture for more than 2-3 weeks due to cell detachment followed by cell death ($p<0.001$). Next, we evaluated the *in vitro* differentiation potential of mFMSC and mEF. For this, both cell types were cultured in commercially available adipogenic, osteogenic and chondrogenic differentiation media. As shown in

figure 1C (left panels), mFMSC displayed a reduced differentiation potential, limited to a low osteogenic commitment, as compared to mEF, which were able to differentiate to both adipogenic and osteogenic lineages. No spontaneous adipogenic or osteogenic differentiation was observed for non-stimulated mFMSC and mEF cultures (figure 1C, right panels). Neither mFMSC nor mEF underwent chondrogenic differentiation upon culture in chondrogenic differentiation medium (data not shown).

Immunomodulating effect of mFMSC and mEF on BV2 microglia

In this part of the study, we aimed to investigate whether mFMSC or mEF could exert an immunomodulating effect on the activation of the C57BL/6-derived BV2 microglial cell line. To this end, we followed the experimental set-up as described in figure 1D (a, upper scheme). As shown in figure 1D (b, lower graph), BV2 cells readily produce high amounts of TNFα upon stimulation with LPS/IFNγ ($p<0.001$ for BV2 vs. BV2+LPS/IFNγ). mFMSC do not produce significant amounts of TNFα, nor upon stimulation with LPS/IFNγ or co-culture with BV2 cells. However, when mFMSC/BV2 co-cultures are stimulated with LPS/IFNγ, a reduced production of TNFα by BV2 cells can be noted ($p<0.001$ for mFMSC+BV2+LPS/IFNγ vs. BV2+LPS/IFNγ). While mEF alone or upon co-culture with BV2 cells do not produce significant amounts of TNFα, stimulation of mEF with LPS/IFNγ leads to a significant increase in TNFα production ($p<0.001$ for mEF vs. mEF+LPS/IFNγ). This observation indicates that, independent of their embryonic fibroblast-like origin, both mFMSC and mEF behave differently upon encounter of immune stimuli. Nevertheless, even though mEF can produce significant amounts of TNFα, in the event of LPS/IFNγ stimulation of mEF/BV2 co-cultures, an overall reduced production of TNFα by BV2 (or mEF) cells can be noted ($p=0.001$ for mEF+BV2+LPS/IFNγ vs. BV2+LPS/IFNγ). Based on the presented data, we conclude that both mFMSC and mEF are able to partially modulate *in vitro* activation of the BV2 microglial cell line.

Differential production of VEGF by mFMSC and mEF under normal and inflammatory conditions

In this part of the study, we investigated the *in vitro* secretion of VEGF by mFMSC and mEF cultures in the absence or presence of (activated) BV2 microglial cells (see figure 1D, (a) upper scheme for experimental set-up). As shown in figure 1E, mFMSC cultures secrete significantly higher levels of VEGF in comparison to mEF cultures ($p<0.001$ for mFMSC vs. mEF). Unexpectedly, in the presence of (activated) BV2 microglia, mFMSC reduce their production of VEGF ($p<0.001$ for mFMSC vs. mFMSC + BV2 and $p=0.004$ for mFMSC vs. mFMSC + BV2 + LPS/IFNγ). In contrast, mEF display an increased VEGF production upon application of pro-inflammatory stimuli ($p<0.001$ for mEF vs. mEF + LPS/IFNγ), which is further increased by the presence of activated BV2 microglia ($p<0.001$ for mEF + LPS/IFNγ vs. mEF + BV2 + LPS/IFNγ). Based on the presented data, we conclude that mFMSC and mEF might display different angiogeneic properties upon *in vivo* grafting into an inflammatory environment.

Quantitative analysis of mFMSC and mEF graft survival following intracerebral transplantation

Next, we aimed to investigate the *in vivo* behaviour of mFMSC and mEF upon autologous grafting in the CNS of immune competent mice. To this end, $5x10^4$ mFMSC-eGFP or $5x10^4$ mEF-eGFP were grafted into the CNS of syngeneic C57BL/6 mice (n=5 for each group). Histological analyses of brain tissue from cell-grafted mice were performed at day 14 post-implantation. For this, cryosections of the whole graft site area were prepared and screened for the presence of eGFP-expressing mFMSC or mEF implants. From the representative images provided in figure 2A, it is clear that eGFP-expressing cellular grafts could be detected 2 weeks after implantation (cell grafts were identified in 4/5 mice transplanted with mFMSC-eGFP and in 5/5 mice transplanted with mEF-eGFP). Notably, the graft site volume (i.e. the volumetric area containing eGFP-expressing cells, figure 2Ba) and the total number of cells within the graft site (comprising both eGFP-expressing grafted cells and microglia, figure 2Bb) is

significantly smaller for mFMSC grafts as compared to mEF grafts (respectively $p<0.001$ and $p=0.002$). Subsequently, it was noted that the number of eGFP+ cells within mFMSC grafts was significantly lower than the number of eGFP+ cells within mEF grafts (figure 2Bb, $p<0.001$). Comparing with the initial number of grafted cells ($5x10^4$ cells), a significantly different degree of cell graft survival was calculated for mFMSC grafts (8% ± 4%) as opposed to mEF grafts (32% ± 14%) (figure 2Bc; $p<0.001$).

Quantitative analysis of glial cell responses following mFMSC and mEF grafting

In our preceding studies regarding mMSC and mEF grafting in the CNS of immune competent mice, we noted that mMSC and mEF grafts became highly infiltrated by microglia (at week 2 post grafting up to 50-80% of cells within the graft site are microglia) and surrounded by microglia and astrocytes. From the representative Iba1/eGFP, S100b/eGFP and GFAP/eGFP images provided in figure 2A, it is clear that mFMSC grafts too become highly infiltrated by microglia and surrounded by both microglia and astrocytes. As shown in figure 2Bb, microglia comprise respectively 75% ± 6% and 58% ± 3% of the total number of cells within a mFMSC and mEF graft site, with the ratio of microglia to eGFP+ cells being significantly higher for mFMSC grafts than for mEF grafts (respectively 2.9±0.8 and 1.5±0.3, $p=0.001$). The latter can however presumably be explained by the lower degree of cell survival observed for mFMSC grafts as compared to mEF grafts. For the graft site surrounding, no difference in density of Iba1+ microglia ($p=0.205$) and S100b+ astrocytes ($p=0.358$) was observed between mFMSC and mEF grafts (figure 2Bd). Additionally, no difference in the degree of GFAP+ astrogliosis was observed around mFMSC and mEF grafts (figure 2Be, $p=0.924$). Therefore, despite the lower degree of mFMSC graft survival as compared to mEF grafts, no differences were observed in both degree and organisation of endogenous glial cell responses.

Quantitative analysis of neo-angiogenesis within mFMSC and mEF grafts

Long-term survival of cellular grafts *in vivo* relies on the ability of the grafted cell type to support neo-angiogenesis. Although the precise mode of action has not yet been fully unravelled, it is well recognized that fibroblasts play a major role in physiological and pathological angiogenesis. Therefore, we additionally determined neo-angiogenesis in mFMSC and mEF grafts. As shown by the representative CD31/eGFP images in figure 2A and their graphical representation in figure 2Bf, a significantly lower blood vessel density was observed within mFMSC as compared to mEF cell grafts ($p<0.001$). This observation is fully in line with our *in vitro* results regarding the respectively reduced/increased VEGF production by mFMSC and mEF under inflammatory conditions (figure 1E).

DISCUSSION

Fibroblastoid cells of mesenchymal origin are considered as highly attractive candidates for cell grafting experiments in the CNS. Although the main aim in this strategy is not direct cell replacement therapy, fibroblast(-like) cells might exert beneficial effects by means of bystander therapy. For example, exploitation of their immune-modulating, regeneration-inducing and/or anti-apoptotic capacity has been well described in multiple pre-clinical disease models of CNS and peripheral injury (1,5,9,25,27). Additionally, mesenchymal cells are attractive candidates as carriers for therapeutic proteins *in vivo*, a strategy that is extensively investigated at the moment (23,26). Nevertheless, little is currently known about the actual *in vivo* fate of the grafted cells. In our preceding studies, we already described that both mMSC and mEF become surrounded and infiltrated by microglia and surrounded by astrocytes. In this study we observed a similar immune recognition pattern *in vivo* using mFMSC as an extra-embryonic mesenchymal cell population. However, our data do highlight several differences between mEF and mFMSC. First, in contrast to mEF, mFMSC do not display proliferation *in vitro*. Currently, we do not have a valid explanation for this observation, although it remains to be elucidated whether the used culture medium for mFMSC can be further optimised. With regard to this matter, it should be noted here that murine foetal membranes are developmentally organised differently compared to human foetal membranes (11), and therefore might benefit from the use of a different expansion medium (in this study we used expansion medium that has proven effective for hFMSC). Second, for our cultured mFMSC we were unable to demonstrate *in vitro* tri-lineage differentiation, a feature that is also under debate for hFMSC (19). However, as mEF displayed differentiation into adipogenic and osteogenic lineage, we believe our *in vitro* differentiation protocol to be satisfactory. Therefore, murine development may have imposed distinct features to mFMSC and mEF/mMSC, despite all being of mesenchymal origin. Further research will have to address this topic. Of note, a recently published study also attributed distinct immunomodulatory and migratory

mechanisms to human mesenchymal cells derived from different tissues (15,20). Third, while mEF cultures are responsive to LPS/IFNγ signalling, mFMSC cultures are unresponsive, at least with regards to TNFα production. Although further investigation will be needed to determine the presence and/or absence of Toll-like receptors on both cell populations and their responsiveness to stimuli of the immune system, the unresponsiveness of mFMSC can potentially be viewed in light of protecting the embryo against inflammatory signalling during maternal inflammation. However, with regard to the intrinsic capacity of mFMSC and mEF to suppress TNFα by activated microglia, we did not observe significant differences between both cell populations. This observation can however be explained by the fact that most – if not all – cells of mesenchymal origin display this feature *in vitro* (13). Fourth, despite the absence of a manifest difference in the *in vivo* immune response triggered against mFMSC or mEF grafts, it was clearly noted that mFMSC display a lower degree of cell graft survival as compared to mEF grafts. Although further research will be needed, our study indicated differences in the capacity of mFMSC and mEF to produce VEGF. The ability to support neo-angiogenesis is a major prerequisite for cell graft survival as – in most cases – cell transplantation is performed without any structural support. Unexpectedly, we first noted that mFMSC produce high levels of VEGF, while mEF do not. However, upon co-culture of mFMSC with (activated) microglial cells, a reduction in VEGF secretion was noted. In contrast, mEF are triggered to produce high levels of VEGF upon co-culture with activated microglial cells. As we have shown in a preceding study that microglia within MSC grafts display an M1-oriented phenotype (10), we here suggest that the activation status of graft-infiltrating microglia might trigger different angiogenic responses in different fibroblast-like cell types, thereby potentially correlating the lower degree of mFMSC graft survival as compared to mEF graft survival. Our work thus implies that further research using advanced cellular and molecular analysis tools will have to reveal the complex signalling between mesenchymal cell grafts, microglia, astrocytes and especially endothelial (progenitor) cells *in vivo*. The latter has also been suggested by *in*

vitro observations describing a crosstalk between mesenchymal stromal cells and endothelial progenitor cells under certain conditions (6,18).

Concluding this study, we have compared the behaviour of mFMSC and mEF *in vitro* and *in vivo* following grafting in the CNS. The presented data indicate significant differences in the ability of both cell populations to respond to inflammatory stimuli, resulting in differential production of TNFα and VEGF under normal and inflammatory conditions. Although further investigation is needed, these apparent differences may lie at the basis of the presence or absence of functional recovery following grafting of different fibroblastoid cell types in animal models of CNS (and other) injuries. Our data thus underscore the need for a thorough characterisation of the cell populations used in cell transplantation studies, as well as the need for comparative cell transplantation studies with similar, but developmentally different, cell populations. Only the latter will lead to a better understanding of the beneficial effects observed in many pre-clinical studies that currently face difficulties when being translated to human clinical applications.

Conflict of interest:

The authors confirm that there are no conflicts of interest.

Acknowledgements:

This work was supported by research grants G.0136.11 and G.0130.11 (granted to ZB and PP) of the Fund for Scientific Research-Flanders (FWO-Vlaanderen, Belgium) and in part by a Methusalem research grant from the Flemish government (granted to ZB and HG). Nathalie De Vocht and Chloé Hoornaert hold a PhD-studentship from the FWO-Vlaanderen. Debbie Le Blon holds a PhD-studentship from the Flemish Institute for Science and Technology (IWT).

References

1. Atoui, R.; Chiu, R. C. Concise review: immunomodulatory properties of mesenchymal stem cells in cellular transplantation: update, controversies, and unknowns. Stem Cells Transl. Med. 1(3):200-205; 2012.
2. Barry, F. P.; Murphy, J. M. Mesenchymal stem cells: clinical applications and biological characterization. Int. J. Biochem. Cell Biol. 36(4):568-584; 2004.
3. Benjamini, Y.; Hochberg, Y. Controlling the false discovery rate - a practical and powerful approach to multiple testing. J. R. Statist. Soc. B. 57(1):289-300; 1995.
4. Bergwerf, I.; De Vocht, N.; Tambuyzer, B.; Verschueren, J.; Reekmans, K.; Daans, J.; Ibrahimi, A.; Van Tendeloo, V.; Chatterjee, S.; Goossens, H.; Jorens, P. G.; Baekelandt, V.; Ysebaert, D.; Van Marck, E.; Berneman, Z. N.; Van der Linden, A. ; Ponsaerts, P. Reporter gene-expressing bone marrow-derived stromal cells are immune-tolerated following implantation in the central nervous system of syngeneic immunocompetent mice. BMC Biotechnol. 9:1; 2009.
5. Bergwerf, I.; Tambuyzer, B.; De Vocht, N.; Reekmans, K.; Praet, J.; Daans, J.; Chatterjee, S.; Pauwels, P.; Van der Linden, A.; Berneman, Z. N.; Ponsaerts, P. Recognition of cellular implants by the brain's innate immune system. Immunol. Cell Biol. 89(4):511-516; 2011.
6. Bidarra, S. J.; Barrias, C. C.; Barbosa, M. A.; Soares, R.; Amedee, J.; Granja, P. L. Phenotypic and proliferative modulation of human mesenchymal stem cells via crosstalk with endothelial cells. Stem Cell. Res. 7(3):186-197; 2011.
7. Bieback, K.; Wuchter, P.; Besser, D.; Franke, W.; Becker, M.; Ott, M.; Pacher, M.; Ma, N.; Stamm, C.; Kluter, H.; Muller, A.; Ho, A. D. Mesenchymal stromal cells (MSCs): science and f(r)iction. J. Mol. Med. (Berl). 90(7):773-782; 2012.
8. Cargnoni, A.; Gibelli, L.; Tosini, A.; Signoroni, P. B.; Nassuato, C.; Arienti, D.; Lombardi, G.; Albertini, A.; Wengler, G. S.; Parolini, O. Transplantation of allogeneic and xenogeneic placenta-derived cells reduces bleomycin-induced lung fibrosis. Cell Transplant. 18(4):405-422; 2009.
9. Dailey, T.; Tajiri, N.; Kaneko, Y.; Borlongan, C. V. Regeneration of neuronal cells following cerebral injury. Front. Neurol. Neurosci. 32:54-61; 2013.
10. De Vocht, N.; Lin, D.; Praet, J.; Hoornaert, C.; Reekmans, K.; Le Blon, D.; Daans, J.; Pauwels, P.; Goossens, H.; Hens, N.; Berneman, Z.; Van der Linden, A.; Ponsaerts, P. Quantitative and phenotypic analysis of mesenchymal stromal cell graft survival and recognition by microglia and astrocytes in mouse brain. Immunobiol. 218(5):696-705; 2013.
11. Dobreva, M. P.; Pereira, P. N.; Deprest, J.; Zwijsen, A. On the origin of amniotic stem cells: of mice and men. Int. J. Dev. Biol. 54(5):761-777; 2010.
12. Evangelista, M.; Soncini, M.; Parolini, O. Placenta-derived stem cells: new hope for cell therapy? Cytotechnol. 58(1):33-42; 2008.
13. Haniffa, M. A.; Collin, M. P.; Buckley, C. D.; Dazzi, F. Mesenchymal stem cells: the fibroblasts' new clothes? Haematologica 94(2):258-263; 2009.
14. Ilancheran, S.; Moodley, Y.; Manuelpillai, U. Human fetal membranes: a source of stem cells for tissue regeneration and repair? Placenta 30(1):2-10; 2009.
15. Liu, K. J.; Wang, C. J.; Chang, C. J.; Hu, H. I.; Hsu, P. J.; Wu, Y. C.; Bai, C. H.; Sytwu, H. K.; Yen, B. L. Surface expression of HLA-G is involved in mediating immunomodulatory effects of placenta-derived multipotent cells (PDMCs) towards natural killer lymphocytes. Cell Transplant. 20(11-12):1721-1730; 2011.
16. Manuelpillai, U.; Moodley, Y.; Borlongan, C. V.; Parolini, O. Amniotic membrane and amniotic cells: potential therapeutic tools to combat tissue inflammation and fibrosis? Placenta 32 Suppl 4:S320-325; 2011.

17. Manuelpillai, U.; Tchongue, J.; Lourensz, D.; Vaghjiani, V.; Samuel, C. S.; Liu, A.; Williams, E. D.; Sievert, W. Transplantation of human amnion epithelial cells reduces hepatic fibrosis in immunocompetent CCl(4)-treated mice. Cell Transplant. 19(9):1157-1168; 2010.
18. Oskowitz, A.; McFerrin, H.; Gutschow, M.; Carter, M. L.; Pochampally, R. Serum-deprived human multipotent mesenchymal stromal cells (MSCs) are highly angiogenic. Stem. Cell? Res. 6(3):215-225; 2011.
19. Parolini, O.; Alviano, F.; Bergwerf, I.; Boraschi, D.; De Bari, C.; De Waele, P.; Dominici, M.; Evangelista, M.; Falk, W.; Hennerbichler, S.; Hess, D. C.; Lanzoni, G.; Liu, B.; Marongiu, F.; McGuckin, C.; Mohr, S.; Nolli, M. L.; Ofir, R.; Ponsaerts, P.; Romagnoli, L.; Solomon, A.; Soncini, M.; Strom, S.; Surbek, D.; Venkatachalam, S.; Wolbank, S.; Zeisberger, S.; Zeitlin, A.; Zisch, A.; Borlongan, C. V. Toward cell therapy using placenta-derived cells: disease mechanisms, cell biology, preclinical studies, and regulatory aspects at the round table. Stem Cells Dev. 19(2):143-154; 2010.
20. Payne, N. L.; Sun, G.; McDonald, C.; Layton, D.; Moussa, L.; Emerson-Webber, A.; Veron, N.; Siatskas, C.; Herszfeld, D.; Price, J.; Bernard, C. C. Distinct immunomodulatory and migratory mechanisms underpin the therapeutic potential of human mesenchymal stem cells in autoimmune demyelination. Cell Transplant. 22(8):1409-1425; 2013.
21. Praet, J.; Reekmans, K.; Lin, D.; De Vocht, N.; Bergwerf, I.; Tambuyzer, B.; Daans, J.; Hens, N.; Goossens, H.; Pauwels, P.; Berneman, Z.; Van der Linden, A.; Ponsaerts, P. Cell type-associated differences in migration, survival, and immunogenicity following grafting in CNS tissue. Cell Transplant. 21(9):1867-1881; 2012.
22. Reekmans, K.; De Vocht, N.; Praet, J.; Fransen, E.; Le Blon, D.; Hoornaert, C.; Daans, J.; Goossens, H.; Van der Linden, A.; Berneman, Z.; Ponsaerts, P. Spatiotemporal evolution of early innate immune responses triggered by neural stem cell grafting. Stem Cell Res. Ther. 3(6):56; 2012.
23. Reekmans, K.; Praet, J.; Daans, J.; Reumers, V.; Pauwels, P.; Van der Linden, A.; Berneman, Z. N.; Ponsaerts, P. Current challenges for the advancement of neural stem cell biology and transplantation research. Stem Cell Rev. 8(1):262-278; 2012.
24. Reekmans, K. P.; Praet, J.; De Vocht, N.; Tambuyzer, B. R.; Bergwerf, I.; Daans, J.; Baekelandt, V.; Vanhoutte, G.; Goossens, H.; Jorens, P. G.; Ysebaert, D. K.; Chatterjee, S.; Pauwels, P.; Van Marck, E.; Berneman, Z. N.; Van der Linden, A.; Ponsaerts, P. Clinical potential of intravenous neural stem cell delivery for treatment of neuroinflammatory disease in mice? Cell Transplant. 20(6):851-869; 2011.
25. Ronsyn, M. W.; Berneman, Z. N.; Van Tendeloo, V. F.; Jorens, P. G.; Ponsaerts, P. Can cell therapy heal a spinal cord injury? Spinal Cord 46(8):532-539; 2008.
26. Ronsyn, M. W.; Daans, J.; Spaepen, G.; Chatterjee, S.; Vermeulen, K.; D'Haese, P.; Van Tendeloo, V. F.; Van Marck, E.; Ysebaert, D.; Berneman, Z. N.; Jorens, P. G.; Ponsaerts, P. Plasmid-based genetic modification of human bone marrow-derived stromal cells: analysis of cell survival and transgene expression after transplantation in rat spinal cord. BMC Biotechnol. 7:90; 2007.
27. Shinozuka, K.; Dailey, T.; Tajiri, N.; Ishikawa, H.; Kim, D. W.; Pabon, M.; Acosta, S.; Kaneko, Y.; Borlongan, C. V. Stem cells for neurovascular repair in stroke. J. Stem Cell Res. Ther. 4(4):12912; 2013.
28. Tambuyzer, B. R.; Bergwerf, I.; De Vocht, N.; Reekmans, K.; Daans, J.; Jorens, P. G.; Goossens, H.; Ysebaert, D. K.; Chatterjee, S.; Van Marck, E.; Berneman, Z. N.; Ponsaerts, P. Allogeneic stromal cell implantation in brain tissue leads to robust microglial activation. Immunol. Cell Biol. 87(4):267-273; 2009.
29. Yu, S.; Tajiri, N.; Franzese, N.; Franzblau, M.; Bae, E.; Platt, S.; Kaneko, Y.; Borlongan, C. V. Stem cell-like dog placenta cells afford neuroprotection against ischemic stroke model via

heat shock protein upregulation. PLoS. One 8(9):e76329; 2013.
30. Zeger, S. L.; Liang, K. Y.; Albert, P. S. Models for longitudinal data - a generalized estimating equation approach. Biometrics 44(4):1049-1060; 1988.

Figure legends

Figure 1: In vitro characterisation of mFMSC and mEF.

(A) Bright field images of *in vitro* cultured mFMSC (a) and mEF (b). The scale bar indicates 200 µm. Inset images: flow cytometric analysis of eGFP expression. Thin line histogram: FL-1 fluorescence of control mFMSC (a) and mEF (b). Bold line histogram: eGFP fluorescence of mFMSC-eGFP (a) and mEF-eGFP (b). Immunophenotypical analysis of mFMSC (c) and mEF (d). Thin line histogram: unstained control. Bold line histogram: specific antibody staining. Representative images were chosen from 2 independent immune phenotyping experiments for mFMSC and mEF. (B) *In vitro* growth of mFMSC(-eGFP) (n=9) and mEF(-eGFP) (n=3) cultures. The counted cell number at plating was set to 1 for data analysis. The values are given as the average ± standard deviation. Results indicate an increase in cell number over time for mEF cultures ($p<0.001$) and a decrease in cell number over time for mFMSC cultures ($p<0.001$). (C) *In vitro* differentiation potential of mFMSC and mEF. Adipogenic differentiation assay: lipid droplets marked by Oil Red O staining for neutral lipids. Osteogenic differentiation assay: calcium deposition evidenced by Alizarin Red staining (scale bar = 100 µm). Representative images were chosen from 2 independent differentiation experiments for mFMSC and mEF. (D) *In vitro* evaluation of immunomodulation properties of mFMSC and mEF. (a) Schematic overview of the experimental outline. (b) Bar chart shows TNFα secretion by BV2 cells alone, after stimulation with LPS/IFNγ and after co-culture with mFMSC or mEF. TNFα production has been quantified by ELISA on cell culture supernatants 24 hours after LPS/IFNγ stimulation. Presented results are given as average ± standard deviation for 2 independent stimulation experiments for mFMSC and mEF, with each experiment performed in quadruplicate (for each condition, n=8). Results indicate: (i) that BV2 cells produce significant levels of TNFα upon stimulation with LPS/IFNγ ($p<0.001$), (ii) that mFMSC reduce the level of TNFα production by LPS/IFNγ-stimulated BV2 cells ($p<0.001$), (iii) that mEF produce significant levels of TNFα upon stimulation with

LPS/IFNγ ($p<0.001$), and (iv) that despite intrinsic potential to produce TNFα, mEF still reduce the level of TNFα production by LPS/IFNγ-stimulated BV2 cells ($p=0.001$). (E) *In vitro* VEGF production by mFMSC and mEF. Bar chart shows VEGF production by mFMSC or mEF alone, after stimulation with LPS/IFNγ in the presence or absence of BV2 cells. VEGF production has been quantified by ELISA on cell culture supernatants 24 hours after LPS/IFNγ stimulation. Presented results are given as average ± standard deviation for 2 independent stimulation experiments for mFMSC and mEF, with each experiment performed in quadruplicate (for each condition, n=8). Results indicate: (i) that mFMSC produce significant levels of VEGF ($p<0.001$), (ii) that both non-activated and LPS/IFNγ-stimulated BV2 cells can suppress VEGF production by mFMSC ($p<0.001$ and $p=0.004$), and (iii) that mEF display an increased level of VEGF production upon stimulation with LPS/IFNγ ($p<0.001$), which is further increased in the presence of LPS/IFNγ-stimulated BV2 cells ($p<0.001$).

Figure 2: Histological analysis of mFMSC-eGFP and mEF-eGFP grafts in the central nervous system of immune competent mice.

(A) Representative immunofluorescent images of the histological analysis of mFMSC-eGFP and mEF-eGFP grafts. Direct eGFP fluorescence (in green) combined with (from left to right): nuclear staining with DAPI (in blue), immunofluorescent staining for microglia (Iba1, in red), astrocytes (S100b, in red), astrogliosis (GFAP, in blue) and blood vessels (CD31, in red) at week 2 post implantation. Representative images were chosen from multiple stained slides (n = 2 for eGFP/Iba1 and eGFP/S100b/GFAP combinations, and n = 1 for eGFP/CD31 combination) per cell graft analysed (n = 4 for mFMSC-eGFP grafts and n = 5 for mEF grafts). The scale bars indicate 100 µm. (B) Quantitative analysis of histological images. For each graph, data are presented as mean ± standard deviation for multiple cell grafts analysed (n = 4 for mFMSC-eGFP grafts and n = 5 for mEF grafts). (a) Graft site volume in mm^3. Significant difference between mFMSC and mEF ($p<0.001$). (b)

Absolute number of Iba1+ microglia (white bars) and eGFP+ cells (black bars) within the graft site. Significant difference between mFMSC and mEF with regard to total cell density ($p=0.002$) and significant difference between mFMSC and mEF with regard to total number of surviving eGFP+ cells. (c) Cell graft survival given in %. Significant difference between mFMSC and mEF ($p<0.001$). (d) Density of Iba1+ microglia (white bars) and S100b+ astrocytes (gray bars) within the implant border. (e) Degree of astrogliosis within the implant border (presented as % coverage based on GFAP staining). (f) Density of CD31+ blood vessels within the implant site. Significant difference between mFMSC and mEF ($p<0.001$).

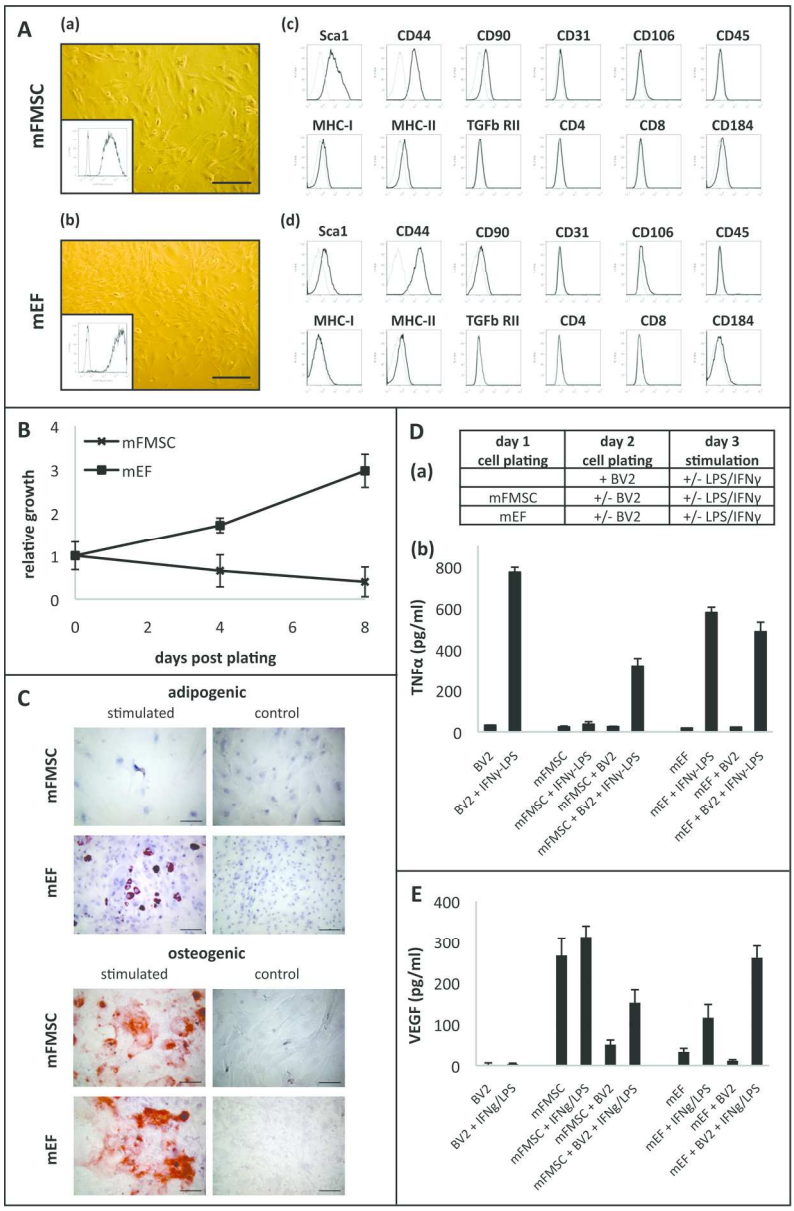

160x243mm (300 x 300 DPI)

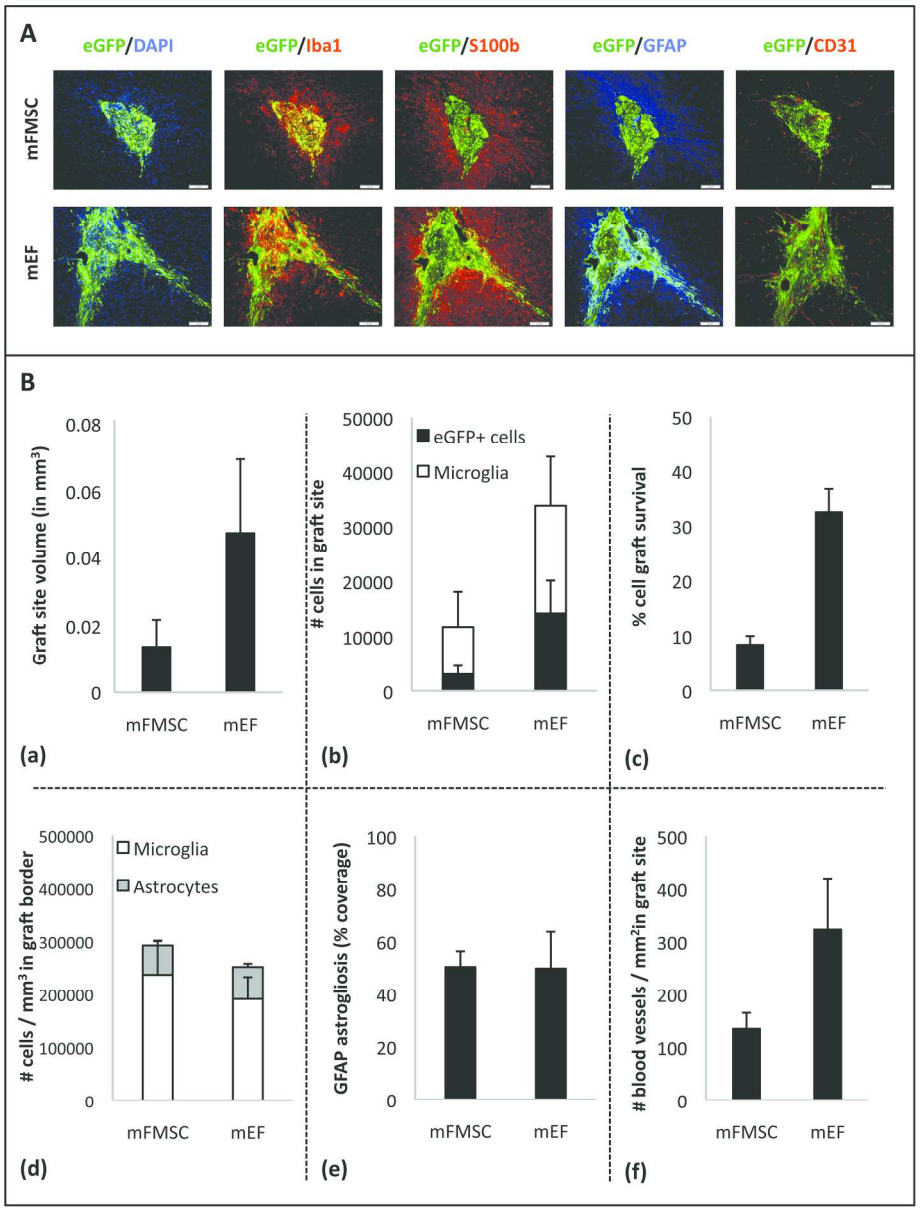

210x277mm (300 x 300 DPI)